Journal of Hazardous Materials B116 (2004) 249–255

Journal of Hazardous Materials

www.elsevier.com/locate/jhazmat

Aerosol particle deposition and distribution in bifurcating ventilation ducts

António F. Miguel[a,b,*], A. Heitor Reis[a,b], Murat Aydin[a,c]

[a] *Geophysics Centre of Évora, Rua Romão Ramalho 59, 7000-671 Évora, Portugal*
[b] *Department of Physics, University of Évora, Apartado 94, 7002-554 Évora, Portugal*
[c] *Mechanical Engineering Department, Istanbul Technical University, 34439 Gumussuyu, Istanbul, Turkey*

Received 22 June 2004; received in revised form 21 September 2004; accepted 25 September 2004
Available online 11 November 2004

Abstract

The quantitative information gained from detailed studies of particle deposition in ducts is important, for example, to evaluate human exposure to particles within buildings, implement cleaning strategies for ventilation ducts and also understand particulate deposition in the respiratory tree. For this purpose, an experimental study for aerosol particles of diameters ranging from 8.1 to 23.2 μm was conducted in a curved bifurcating ventilation duct. At the bend segment of the duct, the particle size, bend angle, curvature ratio and Reynolds number affect aerosol deposition significantly. On the other hand, tests conducted on the bifurcating segments show that deposition increases with particle size and Reynolds number. Accumulation of particles occurs mainly around the bend segment and the ridge of carina of the bifurcation. In all segments of the duct models, particle deposition is found to be enhanced with increasing humidity which increases from 66 to 95% (i.e., close the saturation). A physical interpretation of the results obtained is also presented.

Keywords: Particle deposition; Duct; Bifurcations; Bend; Air humidity; Flow regime

1. Introduction

Particle deposition is of interest to a broadly different areas [1,2]. Aerosols have been identified to come from various sources: environment, equipment activities, smoking, cooking, etc. Malfunctioning of semiconductor [3], erosion in machinery [4] and health effects [5] are some of the important problems caused by deposition of particles. Inhaled particles can deposit in the respiratory tree [6] and trigger significant health problems. These problems can be more serious for people already suffering from respiratory diseases, such as allergy and asthma and cardiovascular problems [1]. Moreover, the presence of particles in air may produce irritation of eyes, nose and throat [7].

Air-conditioning ducts are used in modern buildings with the objective of providing fresh air to indoor environment, control indoor air temperature and, in some cases, also to control indoor pollutants. These ducts play a crucial role in maintaining indoor air quality in large buildings. Their improper functioning may lead to a variety of problems. Aerosol particles can deposit in and re-suspend from the duct surfaces. Re-suspension of particles may expose building occupants to high levels of particle concentration. Besides, deposited particles are known to form a favourable environment for bacteria and fungi growth in presence of water [1,8]. Such growth may lead to: (i) enhancement of bio-aerosol concentrations within the ducts and (2) release of some chemical compounds such as aldehydes into the air stream [9]. Both cases contribute to a deterioration of indoor air quality.

Recently, aerosolized sealant particles have been used to eliminate air leakages in large duct systems [10]. The particles are injected in air with a high level of humidity so that

* Corresponding author. Tel.: +351 266 744616; fax: +351 266 702306.
E-mail address: afm@uevora.pt (A.F. Miguel).

0304-3894/$ – see front matter © 2004 Elsevier B.V. All rights reserved.
doi:10.1016/j.jhazmat.2004.09.013

Nomenclature

C_d	aerosol concentration downstream (m^{-3})
C_u	aerosol concentration upstream (m^{-3})
d	duct diameter (m)
d_p	particle diameter (m)
D	diameter of the curve (m)
De	Dean number
L	duct length (m)
Re	Reynolds number
s	deposition parameter (m^{-2})
u_p	terminal velocity of particle ($m\,s^{-1}$)
U	air velocity ($m\,s^{-1}$)

Greek symbols

α	curvature ratio
η	deposition efficiency
Θ	bend angle
λ	the coefficient takes values either 1/3 or 3/7 depending on flow regime
μ	dynamic viscosity of air (Pa s)
ρ	air density ($kg\,m^{-3}$)
ρ_p	particles density ($kg\,m^{-3}$)
$\dot{\zeta}$	number of particles caught per bend area and second ($m^{-2}\,s^{-1}$)

they deposit in the crack and seal the leak. To ensure that sealant particles reach the intended sites of action, the dose-prediction of the particles is required in this application.

The transport of aerosol particles has not only an exclusive application in engineered duct systems. During inhaling, the gas mixture and particles transported through the respiratory tree may deposit on the duct walls. The importance of understanding particle deposition and retention in the airway system cover the following [1,6]:

(i) Assessing the health hazards of particles: some particles may be captured in the conducting region of the airway system (upper region of respiratory tree), but other particles may reach the gas-exchange surface of the alveolar region. A number of occupational diseases are directly linked to deposition and retention of inhaled particles such as coal, silica, and asbestos. Besides, aerosol particles may damage the mucus layer which covers the conducting region and works as a clearance mechanism for particles.

(ii) Optimal delivery and evaluation of therapeutic effects of pharmaceutical aerosol particles by inhalation (inhalation route drug delivery) in order to reach the predetermined sites in the lung: inhalation of drug aerosol deposited directly to airway target areas results in a reduction of the adverse reactions in the therapy of asthma, and other respiratory disorders.

The extrathoracic region (i.e., airway passage from the nares to larynx) provides heat and moisture to the inhaled air to near body temperature and near water saturation [11].

Aerosol deposition and distribution in ducts can be studied analytically, numerically or experimentally. The use of analytical methods is restricted to simple configurations and they, in most of the cases, suffer from not realistic assumptions [1]. Numerical studies are general and accessible. Numerical investigations were performed for the aerosol deposition in straight ducts and bends (see [1,12,13]). Experimental studies are more expensive and difficult to perform but they provide crucial data to validate analytical and numerical investigations, as well as they make possible to derive empirical relations that are easy to employ.

A small number of experimental investigations devoted to aerosol particle deposition and distribution in ducts can be found in the literature. Among them, Montgomery and Corn [14] studied the deposition of particles (0.44–2.16 μm) in a circular tube of diameter 150 mm in turbulent flow conditions. Saldo et al. [15] and Muyshondt et al. [16] investigated deposition in ducts with different diameters (up to 200 mm). Particle deposition in square and rectangular ducts was studied elsewhere [17–19]. Pui et al. [20] and MacFarland et al. [21] have evaluated deposition in 90° bends for Reynolds numbers between 10^2 and 10^4. Kim et al. [22] reported experimental studies on particle deposition in a single bifurcation duct. Recently, Lai et al. [23] investigated the particle deposition along a rib roughened duct under turbulent conditions.

Real ventilation systems consist of a large duct that branch several times into successively smaller diameter ducts to deliver air to a variety of locations within the building. However, experimental data for aerosol transport and deposition in multi-bifurcated ducts is not found in the literature. Furthermore, we have also noticed that no investigations address the effect of air humidity upon particle deposition. However, it is known that high humidity has a strong influence upon deposition of particles in air filters [24,25].

This work focuses on aerosol particle deposition in double-bifurcating duct with a curved entrance. This duct configuration can be found in many industrial applications, some instruments and also in the upper region of respiratory tree [1,11]. The aim of the current study is to perform quantitative studies on aerosol particle deposition and distribution for the duct configuration with various curvature ratios and bend angles under different levels of air humidity.

2. Materials and methods

The experiments were carried out with the following objectives:

- Assessment of the aerosol particle deposition in different segments of the duct (Experiment #a).
- Qualitative investigation of the distribution of particles deposited within the duct (Experiment #b).

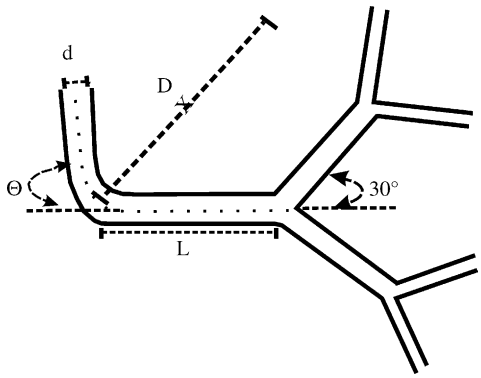

Fig. 1. Schematic representation of ventilation duct model.

The experimental approach taken in this study involves forcing air with suspended particles through the model and the measurement of the particles deposited within the model. The following section summarizes the experimental setup and the procedure used in the study.

2.1. Experimental description

The duct model used for both experiments (#a and #b) is shown in Fig. 1. The setup to create necessary conditions in the experiments is also shown in Fig. 2. Clean air (i.e., air free from particles) kept in an acclimatized container [A] at 26 °C (±2 °C) and relative humidity of 66 and 95% (±4%) was pumped at different flow rates into the model by controlling the rotational speed of the centrifugal fan [B]. Alumina particles, commercially available in a wide range of sizes, were distributed by a particle disperser [C] into the centre of the inlet duct model, in the opposite direction to airflow [D]. Monodisperse particles were used with a geometric standard deviation less than 1.2 and diameters ranging from 8.1 to 23.2 μm.

The velocity of air pumped into the duct model [E] was measured by a calibrated fan [F] placed behind the air supplying fan. The aerosol particle concentration at the different segments of the duct models was obtained by means of a particle size spectrometer which also allows the measurement the aerodynamic diameter of the test particles.

Additional details of setup and procedure can be found elsewhere [24,28].

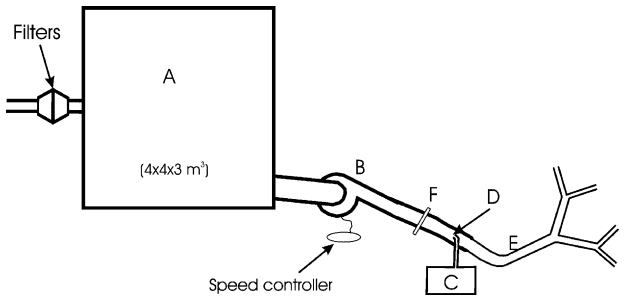

Fig. 2. Schematic representation of the setup.

2.2. Bifurcating duct with a curved inlet

The experiment #a was conducted in the double-bifurcating duct models shown schematically in Fig. 1. These models have the inlet segment curved 0°, 30°, 45° and 90° with horizontal. All ducts were made of Mylar (polyester), the inlet tube is 40 mm in diameter and 400 mm in length (L_0). At each paring node the duct diameter and length presented the following relations:

$$\frac{d_{i+1}}{d_i} = 2^{-\lambda} \tag{1}$$

$$\frac{L_{i+1}}{L_i} = 2^{-\lambda} \tag{2}$$

where d_i and L_i are the diameter and length of each of the two ducts that converge into the duct of diameter and length d_{i+1} and L_{i+1}, respectively. The coefficient λ depends on flow regime and should be taken as 1/3 and 3/7 for fully developed laminar and turbulent flow, respectively. The relations (1) and (2) represent the optimal size step (change in diameter and length) at each pairing node such that the global flow resistance is minimized [1,26,27].

The experiment #b was conducted in a single bifurcating duct model with the inlet segment curved by 90°. The model was cut lengthwise and opened in order to cover its interior with a very thin polyester film. Then, the duct was tested in the setup shown in Fig. 2. In this experiment, monodisperse fluorescent latex particles having a diameter of 10.5 μm were used.

After the experiment, the polyester film was carefully removed and cut into pieces of 50 mm × 50 mm. The particles deposited onto each piece were counted by means of a fluorescent light microscope.

2.3. Evaluation of flow characteristics and aerosol deposition

The particle deposition at different segments of the duct models was determined by measuring the aerosol concentration upstream (C_u) and downstream (C_d) the segment. Then, the deposition efficiency (η) was determined according to

$$\eta = 1 - \frac{C_d}{C_u} \tag{3}$$

Reynolds number (Re) was used to characterize the fluid flow regime in straight ducts and defined as

$$Re = \frac{\rho U d}{\mu} \tag{4}$$

where U is the air velocity, ρ the density and μ the dynamic viscosity of air.

Fluid flow in bends develops a secondary vortex called the double-eddy or Dean's effect which occurs in a plane perpendicular to the main flow [29]. The central part of the flow that has a higher velocity than in the peripheral is de-

viated under the centrifugal force and displaces the slower part of the flow to the center of curvature. Then, a secondary cross-flow (perpendicular to the main flow) emerges there. This secondary flow is present in both laminar and turbulent flow provided that the duct is significantly curved. The strength of this secondary flow depends on the ratio of the curvature of the bend to the tube diameter, flow velocity and fluid properties. A visualization of these phenomena is available elsewhere [30,31].

Dean number is generally used to characterize fluid flow regime in bend ducts and defined as [32]:

$$De = Re\sqrt{\alpha} \tag{5}$$

with

$$\alpha = \frac{d}{D} \tag{6}$$

where α is the curvature ratio, d the tube diameter and D the diameter of the curve.

For the inlet bended Θ with the horizontal (Fig. 1), the flow is controlled by two parameters: Reynolds number and curvature ratio. For a constant α, the centrifugal force increases with fluid velocity and therefore enhances the secondary flow.

Particles travelling in the fluid stream are mostly retained in bends. The variables relevant to particle retention are the so-called characteristic deposition parameter (i.e., the number of particles in characteristic dimension d_p that each second get attached to the bend surface [33]) and the terminal velocity of particles in the centrifugal field. According to this we consider that particle deposition, $\dot{\zeta} = \eta/A$, defined as the number of particles caught per bend area and second ($m^{-2}\,s^{-1}$) could be related with: deposition parameter, s (m^{-2}) and terminal particle velocity, u_p ($m\,s^{-1}$). By invoking Buckingham's Π-theorem we conclude that the particle deposition, $\dot{\zeta}$, is of the form:

$$\Pi = \frac{\dot{\zeta} s^{1/2}}{u_p} \tag{7}$$

where Π is a dimensionless group.

As the deposition parameter is given by [33]:

$$s = \frac{1}{d d_p} \tag{8}$$

and the terminal velocity for a particle in a centrifugal field by [1]:

$$u_p = \frac{\rho_p d_p^2 U^2}{9\mu D} \tag{9}$$

where d_p is the diameter of the particles and ρ_p the particles density. Substituting Eqs. (8) and (9) into Eq. (7), we obtain

$$\eta = \frac{\Pi A \rho_p d^{1/2} d_p^{3/2} U^2}{\mu D} = \frac{\Pi Re A \rho_p d_p^{3/2} U}{\rho d^{1/2} D} \tag{10}$$

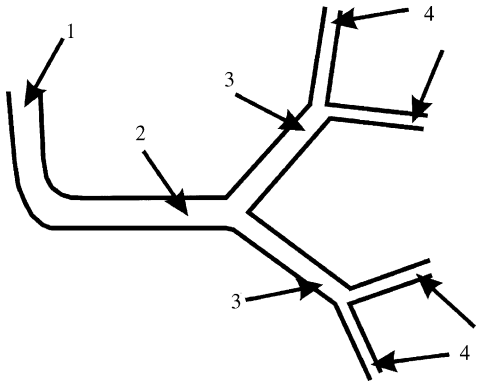

Fig. 3. Measurement locations for the particle number concentrations at the segments of the duct models.

which indicates that the deposition efficiency depends on the characteristics of the bend and particle (d, D, ρ_p, d_p), and fluid velocity (U).

3. Results and discussion

Experiments were performed by measuring the particle concentrations C_u and C_d at different segments of the duct models (Fig. 3).

To find out the deposition of particles at the bend segment, the particle concentration was measured at 1 and 2 (i.e., C_{u1} and C_{d2}). The effects of bend angle, curvature ratio and Dean number upon the deposition efficiency of particles is depicted in Figs. 4–8. Four observations based on these figures follow:

- Deposition efficiency increases with the size of particles. Due to inertia, large aerosol particles hardly adjust themselves to abrupt change in the flow trajectory that occurs in the duct bends and they are intercepted by duct wall.
- Particle deposition increases with increasing bend angle and the Reynolds number. In bends, the emergence of centrifugal forces generates a secondary cross-flow that enhances aerosol particle deposition. A substantial amount

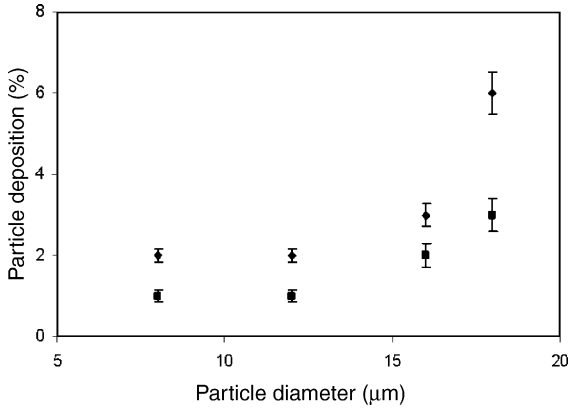

Fig. 4. Particle deposition efficiency in a 30° bend for the curvature ratio of 0.05 (♦) and 0.1 (■). The volumetric flow rate is $1.86 \times 10^{-2}\,m^3/s$.

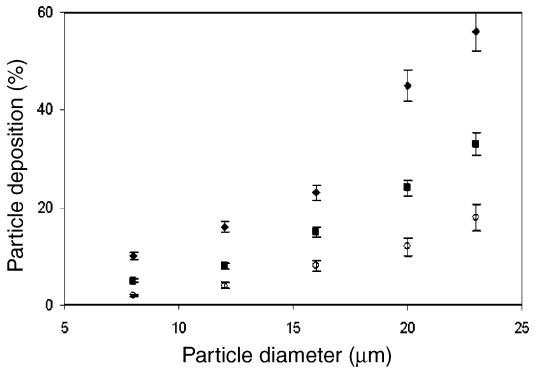

Fig. 5. Particle deposition efficiency in a 60° bend for the curvature ratio of 0.05 (♦), 0.1 (■) and 0.25 (◯). The volumetric flow rate is 1.86×10^{-2} m^3/s.

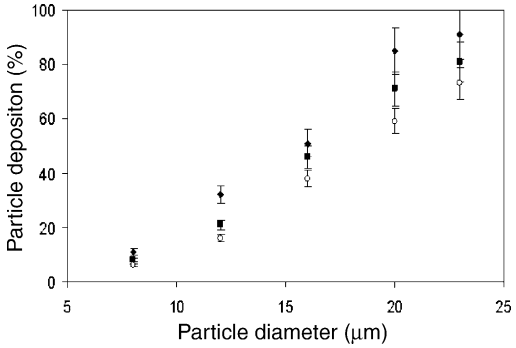

Fig. 6. Particle deposition efficiency in a 90° bend for the curvature ratio of 0.05 (♦), 0.1 (■) and 0.25 (◯). The volumetric flow rate is 1.86×10^{-2} m^3/s.

of fluid (i.e., air and particles) is moved from the centre of the duct to the wall, therefore facilitating the interception of particles by the wall.

- η decreases with increasing curvature ratio. As inlet tube diameter was fixed (40 mm), the enhancement of curvature ratio leads to a smaller path length of the air containing the aerosols. As a result, less collector surface is available for aerosol particles and therefore, less deposition occurs.

Regression analysis of the results presented in Figs. 4–8 shows that the deposition efficiency can be fitted with an equation of the type $\eta \sim d_p^n$ where n takes value between 1.4

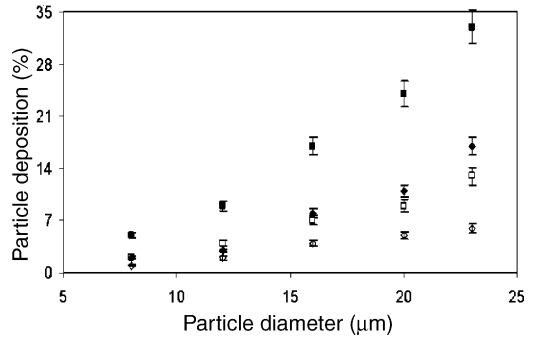

Fig. 7. Particle deposition efficiency in a bend with the curvature ratio of 0.1. (Bend angle is 60°: Re = 1423, De = 450 (◊); Re = 3116, De = 1000 (□). Bend angle is 90°: Re = 1423, De = 450 (♦); Re = 3116, De = 1000 (■).)

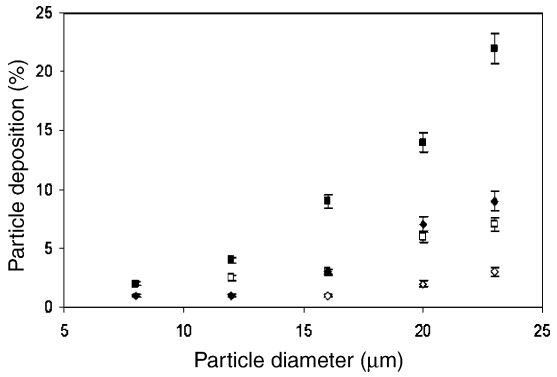

Fig. 8. Particle deposition efficiency in a bend with curvature ratio of 0.25. (Bend angle is 60°: Re = 1423, De = 711 (◊); Re = 3116, De = 1558 (□). Bend angle is 90°: Re = 1423, De = 711 (♦); Re = 3116, De = 1558 (■).)

and 1.8. This tendency is different to that suggested by Pui et al. [20] (they suggest that η varies exponentially with the diameter of the aerosol particles) but is in agreement with Eq. (10). Our results are also different to those given by Pui et al. [20]. They have found no effect of Reynolds number and the curvature ratio on particle deposition. In this matter, our results agree with Eq. (10) and also with numerical results obtained by several authors (see for example [13]).

Notice that, the results presented in Figs. 4–6 clearly reveal that, for bend angles less than 30°, the curvature has a small effect upon deposition of aerosol particles.

Tests conducted on the bifurcating segments yield the results shown in Figs. 9 and 10. Particle deposition at the first and second bifurcations (Fig. 3) was obtained by measuring particle concentration at 2 and 3 (i.e., C_{u2} and C_{d3}), and 3 and 4 (i.e., C_{u3} and C_{d4}), respectively. For all cases, η increases with the particle size and Reynolds number. The reason is that, large particles and particles animated of large velocities experience difficulty to adjust their trajectories to the abruptly changing streamlines in the neighbourhood of the carina. Therefore, the probability of hitting the duct walls is greatly enhanced.

The data presented in Figs. 9 and 10 show that the variation of deposition efficiency with particle diameter is of the form

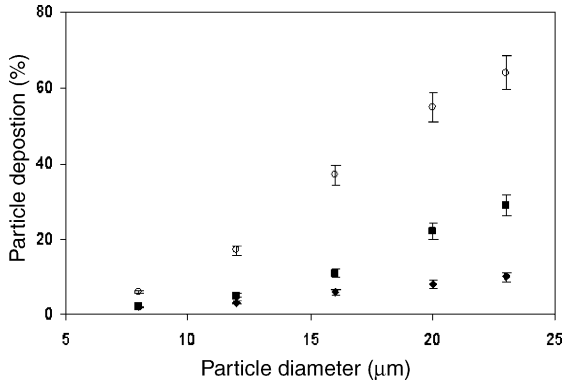

Fig. 9. Particle deposition efficiency at the first bifurcation for different local Reynolds number (Re = 660 (♦), Re = 1422 (■), Re = 3151 (◯)).

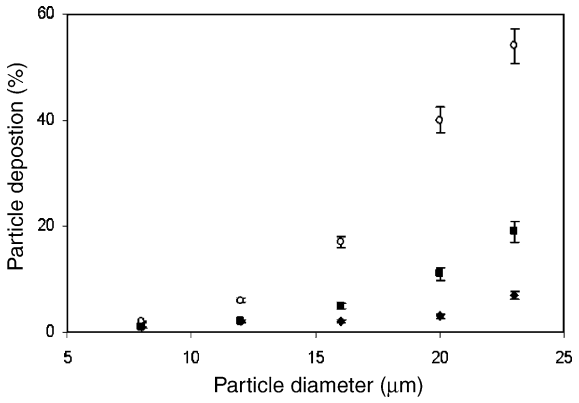

Fig. 10. Particle deposition efficiency at the second bifurcation for different local Reynolds number ($Re = 503$ (♦), $Re = 1066$ (■), $Re = 2335$ (◯)).

$\eta \sim d_p^n$ where the exponent n is between 1.5 and 2.9. Besides, particle deposition at the first bifurcation is higher than that in the second bifurcation. This is due to the fact that the second bifurcation has geometric characteristics (diameter and length) smaller than those of the first bifurcation (see Eqs. (1) and (2)). Consequently, the surface area of the duct available for aerosol particles in the second bifurcation is lower and therefore, deposition efficiency is lower too.

The influence of relative air humidity on the deposition efficiency is shown in Figs. 11–13. In all segments of duct models particle deposition is found to be enhanced when the humidity increases from 66 to 95%. The increase in the deposition efficiency varies between 10 and 35%. When the humidity is near saturation, the particles that hit the duct walls are more likely captured. This is consistent with other results that found that particles adhesion to surfaces increases with the air humidity [24,34].

Local particle deposition patterns (experiment #b) within the bifurcation duct flow having an inlet curved with 90° is reproduced in Fig. 14. The plot reveals that the major particle accumulation occurs around the bend inlet segment and in the carinal ridge. This can be due to inertial effect, i.e., larger particles hardly adjust their trajectories to the abruptly

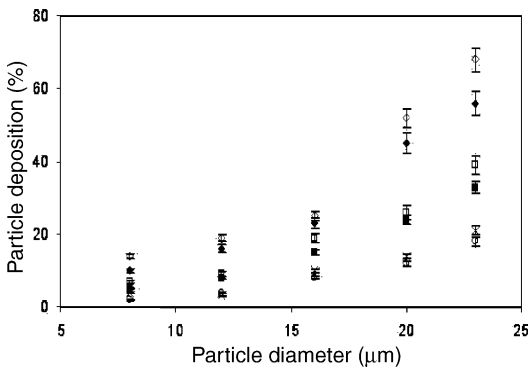

Fig. 11. Effect of air humidity on particle deposition efficiency in a 60° bend for the curvature ratio of 0.05 (humidity 66% (♦), humidity 95% (◊)), 0.1 (humidity 66% (■), humidity 95% (□)) and 0.25 (humidity 66% (◯), humidity 95% (×)). The volumetric flow rate is 1.86×10^{-2} m^3/s.

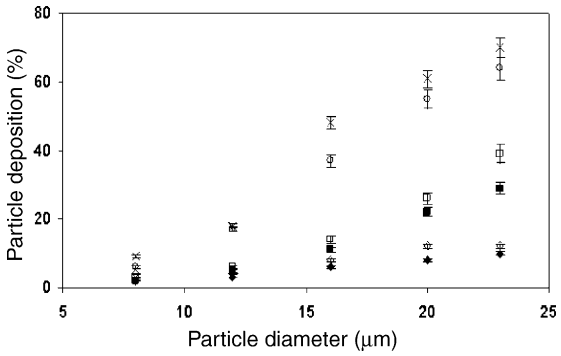

Fig. 12. Effect of air humidity on particle deposition efficiency at the first bifurcation for different Reynolds numbers: $Re = 650$ (humidity 66% (♦), humidity 95% (◊)), $Re = 1422$ (humidity 66% (■), humidity 95% (□)) and $Re = 3151$ (humidity 66% (◯), humidity 95% (×)).

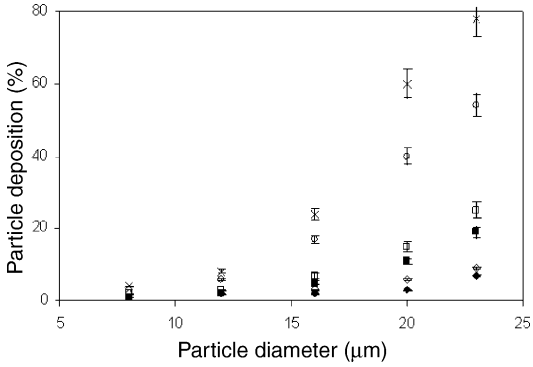

Fig. 13. Effect of air humidity on particle deposition efficiency at the second bifurcation under different Reynolds numbers: $Re = 503$ (humidity 66% (♦), humidity 95% (◊)), $Re = 1066$ (humidity 66% (■), humidity 95% (□)) and $Re = 2335$ (humidity 66% (◯), humidity 95% (×)).

changing streamlines close to the inlet curvature near the carina. Therefore, the probability of hitting the duct walls and being captured for a large particle is greatly enhanced. Besides, secondary foci of deposition are visible after the main deposition area at the part of the bend and following the carinal ridge at the bifurcation but on the opposite side of the duct. We think that these foci may be due to eddies occurred in these locations [31].

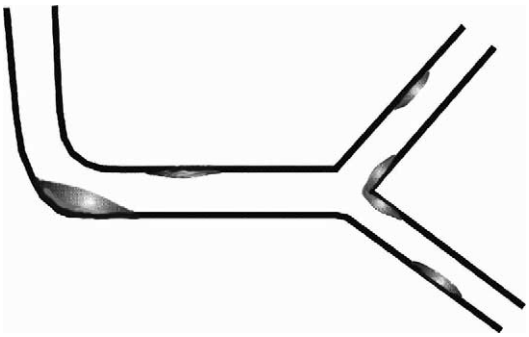

Fig. 14. Schematic representation of the sites of major accumulation of particles within a single bifurcating ventilation duct with the inlet segment curved to 90° ($\alpha = 0.25$).

4. Conclusions

This paper presents new experimental results for the aerosol particle deposition in double-bifurcating ventilation ducts with a bend inlet. Experiments were conducted with monodisperse particles in the 8.1–23.2 μm size range. We found that the aerosol deposition is greatly influenced by the particle size, geometric characteristics of the duct (curvature ratio and bend angle, bifurcations), air humidity level, in addition to the Reynolds number. Besides, major particle accumulation occurs around the bend inlet segment and also in the carinal ridge. The discussion of the results obtained is made on physical grounds.

The importance of the present study is two-fold: (1) allows a better understanding of aerosol particle deposition in ventilation ducts and provides useful information for the design and maintenance of such duct systems; (2) the experiments with a high level of humidity may also contribute to: (i) efficient use of the technique to eliminate air leakages from large duct systems through aerosolized sealant particles [10], and (ii) understanding process of aerosol deposition in the upper region of respiratory tree [1].

Acknowledgements

The authors are grateful to Foundation for Science and Technology (FCT), for providing financial support to carry out the above mentioned experiments (project POCTI/33012/EME/2000).

References

[1] A. Bejan, I. Dincer, S. Lorente, A.F. Miguel, A.H. Reis, Porous and Complex Flow Structures in Modern Technologies, Springer-Verlag, New York, 2004.
[2] R. Tsai, Z.Y. Lin, An approach for evaluating aerosol particle deposition from a natural convection flow onto a vertical flat plate, J. Hazard. Mater. B 69 (1999) 217–227.
[3] A. Litvak, A.J. Gadgil, W. Fish, Hygroscopic fine mode particle deposition on electronic circuits and resulting degradation of circuit performance: an experimental study, Indoor Air 10 (2000) 47–56.
[4] C.E. Smeltzer, M.E. Gulden, W.A. Compton, Mechanisms of metal removal by impacting dust particles, ASME 69 (1969) (WA/Met-8).
[5] E.J. Bardana, A. Montanaro (Eds.), Indoor Air Pollution and Health, Marcel Dekker, New York, 1997.
[6] A.F. Miguel, A.H. Reis, M. Aydin, A.M. Silva, Particle deposition in airway bifurcations in different breathing conditions, J. Aerosol Sci. (European Aerosol Conference) 2 (2004) S1125–S1126.
[7] L. Mϕlhave, S.K. Kjaergaard, J. Attermann, Effects in the eyes caused by exposure to office dust, Indoor Air 12 (2002) 165–174.
[8] M.R. Sippola, W.W. Nazaroff, Modeling particle deposition in ventilation ducts, in: Proceedings of the Ninth Conference on Indoor Air Quality and Climate, 2002, pp. 1811–1819.
[9] P. Pasanen, J. Salo, M. Hyttinen, M. Vartiainen, P. Kalliokoski, Ozone reduction in supply air filters, in: Proceedings of the Healthy Buildings 2000, Helsinki, Finland, 2000, pp. 263–268.
[10] M.P. Modera, O. Brzozwski, F.R. Carrié, D.J. Dickerhoff, W.W. Delp, W.J. Fisk, R. Levinson, D. Wang, Sealing ducts in large commercial buildings with aerosolized sealant particles, Energy Buildings 34 (2002) 705–714.
[11] R. Sarangapani, A.S. Wexler, Modeling particle deposition in extrathoracic airways, Aerosol Sci. Technol. 32 (2000) 72–89.
[12] J.B. McLaughlin, Aerosol particle deposition in numerically simulated channel flow, Phys. Fluids A 1 (1989) 1211–1224.
[13] C.J. Tsai, D.Y.H. Pui, Numerical study of particle deposition in bends of a circular cross-section-laminar flow regime, Aerosol Sci. Technol. 12 (1990) 813–831.
[14] T. Montgomery, M. Corn, Aerosol deposition in a pipe with turbulent air flow, Aerosol Sci. 1 (1970) 185–213.
[15] B. Saldo, E. Verloo, T. Akbiol, F. Sabathier, Study of aerosol deposition in large pipes, J. Aerosol Sci. 25 (1994) S267–S268.
[16] A. Muyshondt, N. Anand, A.R. McFarland, Turbulent deposition of aerosol particles in large transport tubes, Aerosol Sci. Technol. 24 (1996) 107–116.
[17] W. Kvasnak, G. Ahmadi, R. Bayer, M. Gaynes, Experimental investigation of dust particle deposition in a turbulent channel flow, J. Aerosol Sci. 24 (1993) 795–815.
[18] N. Adam, P. Everitt, S.B. Riffat, Aerosol deposition in ventilation ducts, Int. J. Energy Res. 20 (1996) 1095–1101.
[19] K.W. Cheong, Deposition of aerosol particles in ductwork, Appl. Energy 57 (1997) 253–261.
[20] D.Y.H. Pui, F. Romay-Novas, B.Y.H. Liu, Experimental study of particle deposition in bends of circular cross section, Aerosol Sci. Technol. 7 (1987) 301–315.
[21] A.R. MacFarland, H. Gong, A. Muyshondt, W.B. Wente, N.K. Anand, Aerosol deposition in bends with turbulent flow, Environ. Sci. Technol. 31 (1997) 3371–3377.
[22] C.S. Kim, D.M. Fisher, D.J. Lutz, T.R. Gerrity, Particle deposition in bifurcating airway models with varying airway geometry, J. Aerosol Sci. 25 (1994) 567–581.
[23] A.C.K. Lai, M.A. Byrne, A.J.H. Goddard, Enhanced particle loss in ventilation duct with ribbed surface, Building Environ. 35 (2000) 425–432.
[24] A.F. Miguel, Effect of air humidity on the evolution of permeability and performance of a fibrous filter during loading with hygroscopic and non-hygroscopic particles, J. Aerosol Sci. 34 (2003) 783–799.
[25] A.F. Miguel, A.M. Silva, Experimental study of aerosol mass loading behaviour of fibre filters, J. Aerosol Sci. 32 (2001) S851–S852.
[26] R. Rosa, A.H. Reis, A.F. Miguel (Eds.), Bejan's Constructal Theory of Shape and Structure, CGE-UE Press, 2004.
[27] A.H. Reis, A.F. Miguel, M. Aydin, Constructal theory of flow architecture of the lungs, Med. Phys. 31 (2004) 1135–1140.
[28] A.F. Miguel, Contribution to flow characterisation through porous media, Int. J. Heat Mass Transf. 43 (2000) 2267–2272.
[29] C.R. Ethiery, S. Prakah, D.A. Steinman, R.L. Leask, G.G. Couch, M. Ojha, Steady flow separation patterns in a 45 degree junction, J. Fluid Mech. 411 (2000) 1–38.
[30] S.A. Berger, L. Talbot, L.S. Yao, Flow in curved pipes, Annu. Rev. Fluid Mech. 15 (1983) 461–512.
[31] X.Y. Luo, J.S. Hinton, T.T. Liew, K.K. Tan, LES modelling of flow in a simple airway model, Med. Eng. Phys. 26 (2004) 403–413.
[32] T.K. Palazoglua, K.P. Sandeep, Effect of tube curvature ratio on the residence time distribution of multiple particles in helical tubes, Lebensm. Wiss. u. Technol. 37 (2004) 387–393.
[33] A.H. Reis, A.F. Miguel, M. Aydin, Analysis of filter performance as function of particle diameter, filter internal surface and filter pore size distribution, in: Proceedings of the International Conference of Applications of Porous Media ICAPM2004, 2004, pp. 397–400.
[34] W. Höflinger, Fundamentals of the compression behaviour of dust filter cakes, in: K.R. Spurny (Ed.), Advances in Aerosol Filtration, Lewis Publishers, Chelsea, 1998, pp. 349–360.